MECH 499: CNC QC Machine Design and Testing

Dallin Low
V00840277
August 13, 2020

Table of Contents

Summary 3
1 Background 4
2 Objectives/Scope 4
3 Mechanical Design 5
4 Electrical Design 10
5 Firmware Design 12
6 Open-Loop Control Design 13
7 Final Assembly 16
8 Testing Methodology 17
8.1 VL53L0X Material Surface Test 17
8.2 Surface Baseline Scanning Test 18
8.3 Test Piece Flaw Identification 19
9 Testing Results 20
9.1 VL53L0X Material Surface Test 20
9.2 Surface Baseline Scanning Test 21
9.3 Test Piece Flaw Identification 22
10 Discussion 24
11 Conclusion 24
12 References 25

Summary

Geometric quality control (QC) is necessary in all engineering and manufacturing companies regardless of size, however no commercial automated general QC options appear available for low through-put firms. Leveraging the decrease part price of low stress CNC (LSCNC) machines such as 3D-printers the designers purpose during this project is to create a QC CNC machine which employs a laser measurement sensor to scan a 3-axis machined part for comparison with its associated CAD file.

To create this machine the designer based his design off traditional 3D printers. Similarly, the electronics used in this project were common off the shelf parts configured uniquely to produce the novel machine. The firmware created for this project was also custom, and the basics of trajectory generation and open-loop stepper control are discussed.

After designing and assembling the QC CNC machine, its accuracy was tested by scanning preprinted test pieces one of which exhibited small deviations from the CAD file. These scans were then observed empirically to determine the viability of this QC method. From these observations it was determined that though the mechanical, electrical, and firmware design were all sufficiently robust to produce accurate measurements, the implementation of a low-quality laser range-finder sensor resulted in unreliable scanning information.

The designer concludes that his machine was not able to produce sufficiently accurate measurements or scans according to his design goals. He recommends that future QC CNC machines employ industrial grade laser sensors, while continuing to employ the low cost LSCNC parts.

1 Background

Geometric quality control (QC) is an essential step in engineering manufacturing which is ubiquitous among mechanical engineering firms due to recent demands for increased quality and repeatability in products [1]. The process of QC involves scrutinizing designed and ordered mechanical components against the design drawings to ensure that no errors were performed by the manufacturer. This process historically in all but the largest engineering and manufacturing firms with extremely high through-put has been performed by hand, and current automation solutions for generalized QC are incredibly costly (i.e. CNC Touch Probes [11]; require a CNC mill to use).

Previous studies have demonstrated the feasibility of using laser scanning in place of probing on a 3-5 axis CNC milling machine for general QC purposes [10]. Considering no contact control is necessary for this type of probing, the use of this technique could lead to cheaper QC options if paired with low-stress CNC (LSCNC) machines, the parts and controllers of which are ever-decreasing in price due to the increased popularity of desktop Fused Deposition Modeling (FDM) 3D-printers. Under this hypothesis, the designer saw a feasible QC automation option in creating a 2-3 axis CNC machine which used a laser range finder or similar technology in place of an extruder. This machine would receive XY position information as input commands, and measure and transmit the recorded Z-position. This Z-position would then be compared against the desired Z-position in post-processing.

2 Objectives/Scope

The objective of this project was to design and build a CNC QC machine proof of concept prototype within the price range of small-medium sized engineering firms and which was able to accurately preform a QC check at relatively quick speeds. This project only focused on performing QC on parts which could be produced on a 3 axis CNC mill using only one fixturing process. To save resources and project time, as many required components as possible were sourced rather than designed, which included all electronic components. Designs outside of the scope outlined in the *Background* section of this document were not here considered. The design and scope goals are formalized in Table 1.

Table 1 – Design Goals		
Goal	**Units**	**Range**
Cost of functioning prototype	$	<1000
Speed of QC Process	Min	<4
Z-Height Accuracy	mm	±0.1
X/Y Resolution	mm	<1
Time Frame	Dates	May 1 – August 7, 2020

3 Mechanical Design

In order to perform the mechanical conceptual design, several choices, all associated options of which are common in LSCNC design, needed to be made. These options are represented in Table 2.

Table 2 – Design Options

Criteria	Option 1	Option 2	Option 3
Number of Axes	2	3	
Movement System	Belts	Lead Screws	Mixed
Structural Members	2020 Aluminum T-Bar	T-Bar & Cylindrical Members	
Structural Design	T-Type Cartesian	I3-Type Cartesian	
Bearing System	Linear Rails	Cylindrical Bearings	Preloaded Wheels
Use of Encoders	Yes	No	

3.1 Number of Axes

The QC CNC machine being designed would only need to move during scanning in the XY plane given the scope of the project (Z distances would be measured and recorded). However, during preliminary research, it was determined that the low-cost laser range finders available have a field of view characteristic, in which the laser area increases with distance. It was presumed that measurement error would increase with laser area, however no sources for how these two parameters correlate could be determined. The designer hypothesized that any variance in height within the laser area would be averaged during the measurement.

To decrease the laser area as much as possible it was determined that 3-axes would be necessary. Further testing would be carried out to determine the necessity of this design feature.

Equation 1 – Field of view calculations

$FOV = 25°$

$d_{surf}[Distance\ from\ suface] = ??$

$LD\ [Max\ Laser\ diameter\ within\ XY\ resolution\ distance] = 1mm$

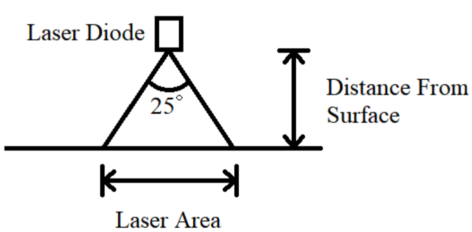

$$d_{surf} = \frac{LD}{2\tan\left(\frac{25°}{2}\right)} = 2.26mm$$

Result: Such a close surface distance would not be possible without variable z height.

**Calculation uses FOV value for VL53L0X sensor [12].

3.2 Movement System

In cartesian LSCNC stepper driven belts and lead screws are the most commonly used methods of axis movement [2]. Belts are light and typically much cheaper than lead screws particularly as a LSCNC gets larger. Belts are unsuitable to drive axes which encounter load due to stretching and slipping, and therefore cannot be used in the z-direction. Lead Screws are heavier and more expensive at large lengths but produce less slipping and higher resistance to load. Knowing that at least one of the three axes would require a lead screw, and to decrease project complexity, it was determined that lead screws would only be used.

This decision was scrutinized against the X/Y Resolution design goal according to the calculations below:

Equation 2 – X/Y Resolution Check

$Step\ length = 1.8°/step$

$microstepping = \frac{1}{8} step$

$Lead\ [T8\ Lead] = \frac{8mm}{360°}$

$Res_{XY}\ [Desired\ XY\ Resolution] = 1mm$

$$Min\ Resolution = \frac{8mm}{360°} * \frac{1.8°}{step} * \frac{1}{8} step = 0.005mm\ or\ 200steps/mm$$

Results:

**Calculation uses specs from Nema17 steppers [13]

3.3 Structural Members

LSCNC machines often use T-bar aluminum members because they do not require any machining before assembly. Cylindrical members are also common particularly when cylindrical bearings are used for axis movement. To simplify assembly and machining, it was decided that only 2020 T-bar and 2040 T-bar members would be used.

3.4 Structural Design

LSCNC machines, particularly FDM 3D-printers, come in a variety of structural designs and control schemes. However, most intuitive and common are cartesian controls in which the kinematics of each axis is decoupled from the other [2]. Two structural cartesian configurations – T-Type and i3-Type – chosen as likely candidates are displayed in Figure 1.

Figure 1 – Two cartesian configurations for consideration – T-Type and i3-Type

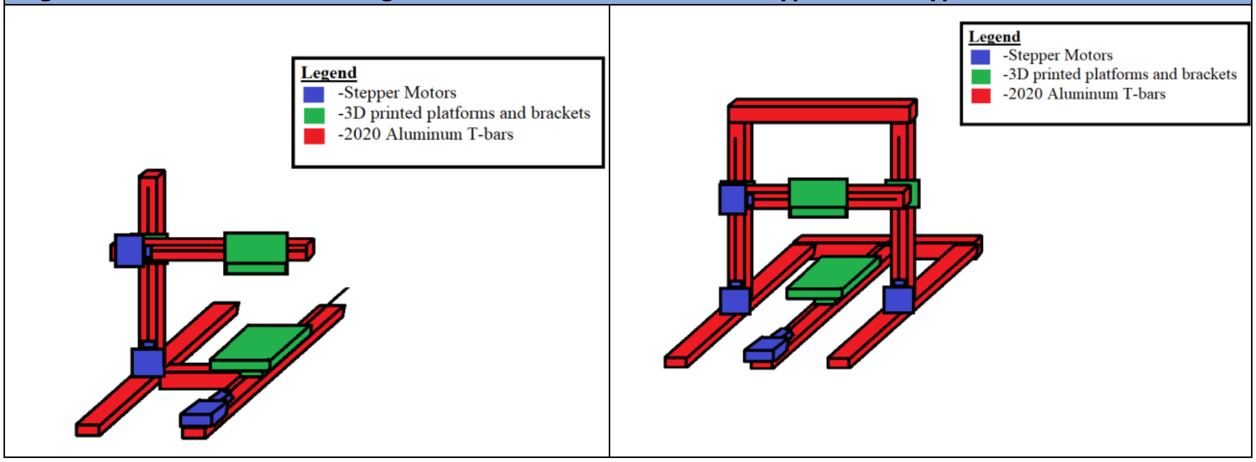

A T-Type LSCNC has price and simplicity advantages simply due to the lack of materials needed for assembly, while i3-Type LSCNC display more robust structural properties. Due to a suspected decrease inaccuracy of the forward kinematics of the X-axis in the T-Type model because of bending, an i3-Type configuration was chosen. Equation 3 demonstrates that either configuration with the specified motors would have been sufficient in holding the X-axis assembly.

Equation 3 – Required Holding Strength (adapted from [3])

$D\ [T8\ Diameter] = 8mm$

$Lead\ [T8\ Lead] = \frac{8mm}{360°}$

$m_{Xaxis}\ [estimated\ mass\ of\ X - axis\ assembly] = 1.233kg$

$T_{mot}\ [motor\ Torque] = 0.40\ Nm$

$MA\ [Mech.Advantage]$

$VR\ [Velocity\ Ratio]$

$\xi\ [Efficiency] = 1\ (an\ assumption)$

$n\ [number\ of\ motors\ required]$

$$MA = VR * \xi = \frac{\pi D}{Lead} = \pi$$

$$MA = \frac{F_{grav}}{F_{Motor}} \rightarrow F_{Motor} = \frac{m * g}{MA} = 3.85N$$

$$T_{Required} = F_{Motor} * \frac{D}{2} = 0.0154\ Nm$$

$$T_{mot} * n \geq T_{Required}$$

$$n_{min} = 1$$

Results: Either motor configuration sufficient for project needs

**Calculation uses specs from Nema17 steppers [13]

3.5 Bearing System

The most common types of bearing systems in LSCNC machines are loaded wheels, cylindrical bearings, and linear tracks [4]. Cylindrical bearings by far produce the most stability for axis movement because each axis is rigidly connected to the rail, however integration of cylindrical bearings would introduce a much higher part count and higher required tolerances of carriages. Linear tracks would provide a much simpler integration at a much higher price. Loaded wheels were in the end chosen due their low costs.

3.6 Use of Encoders

Stepper motors are the most widely used motors in LSCNC machines for a variety of reasons: they are capable of producing a holding torque when stationary, they are widely available, and they are relatively low cost. However, a major disadvantage of common stepper motors is that they are open loop devices, meaning that they do not have any mechanical encoding feedback [5]. For control purposes this can be a major issue if vibrations, high speeds, or stress on any axis of the LSCNC machine produce forces greater than the holding torque, which will cause the steppers to lose track of its angular position (called layer shifting in FDM 3D-printing [6]). To minimize this effect, closed-loop steppers or mechanically connected optical encoders can be employed.

Due to a lack of budget, design time, and under the understanding that the QC CNC would be a low stress machine, it was decided that closed loop feedback would not be employed. It was, however, noted that the use of open loop control would reduce the maximum speed of the machine [14].

3.7 Final Mechanical Design

After completing the above design decisions, a model of the QC CNC machine assembly was completed (see Figure 2).

Figure 2 – Final Mechanical Design Model

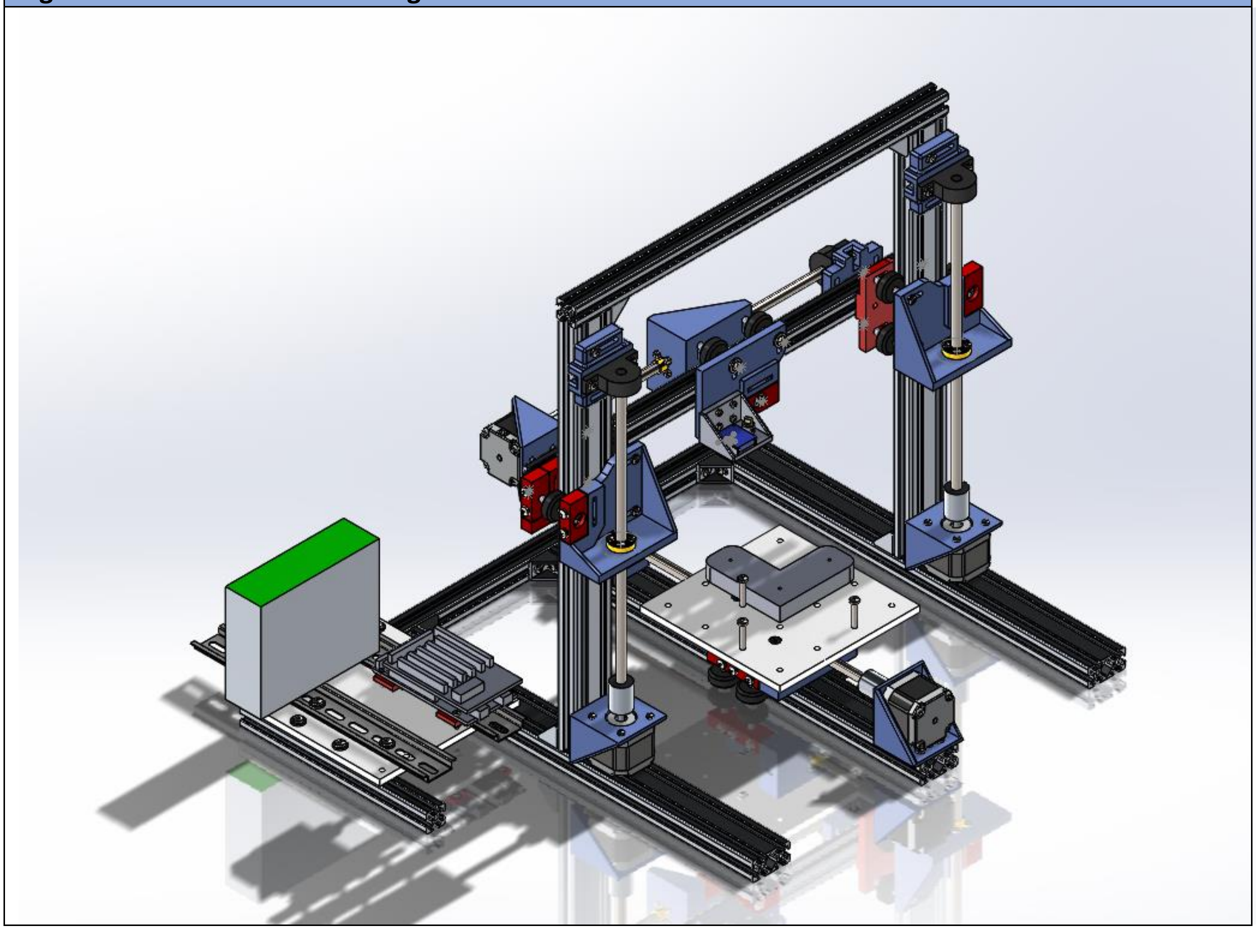

4 Electrical Design

After the completion of the mechanical analysis and design, the electronics of the QC CNC machine were designed and ordered. As stated previously, electronic board design is outside of the scope of this project, and therefore all boards and electronic components were sourced from vendors. Any decision-making processes associated with the design process are listed in the following subsections.

Table 3 – Electrical Design Options			
Criteria	**Option 1**	**Option 2**	**Option 3**
Controller	MKS	Arduino Mega + Ramps 1.4	AutomationDirect P1AM-100 PLC
Distance Sensors	VL53L0X	VL53L1X	KEYENCE Spectral-interference Laser Displacement Meter

4.1 CNC Controller

Given the relatively novel requirements of the QC CNC device, it was necessary to choose an open source programmable CNC controller. Popular options within this category are the smoothieware MKS controller, and the Arduino Mega controller with a Ramps shield [7], both of which are programmed in C and which typically run a customizable 3D-printer firmware called Marlin. To increase industrial compatibility and durability the designer also considered using a C based PLC from AutomationDirect [8], however, to decrease cost this option was abandoned. Eventually the Arduino Mega was chosen due to its output and formfactor versatility compared to the MKS which is optimized for 3D-printing specifically.

4.2 Distance Sensors

Essential to the purposes of this project, the attached distance sensor needed to be:

- Low-cost (<$50)
- As accurate as possible (as specified previously ideally within ±0.1mm)
- Easily integratable into the chosen controller

After considerable research, few sensors were able to fulfill all of the above criteria, particularly with high enough accuracy to be viable options. Some industrial sensors appear to have greater than required precision [9], and with an estimated cost of $1500, could be within the budget of a low to medium throughput engineering company. Given the limited budget of this project however, the designer chose to implement a VL53L0X range-finder sensor, with an accuracy of approximately ±3% [12], which at the calculated clearance distance d_{surf} of 2.26mm would produce a reading with an accuracy of ±0.07mm.

4.3 Final Electrical Design

After completing the above design decisions and ordering the required parts the electronics were connected to the assembled machine (see Figure 3). It should be noted that A4988 stepper drivers were employed for ease of compatibility, a visible laser was attached to ease positioning, and all of the electronics were powered by a 12V power supply.

Figure 3 – Mounted Controller (Left) and Sensor (Right)

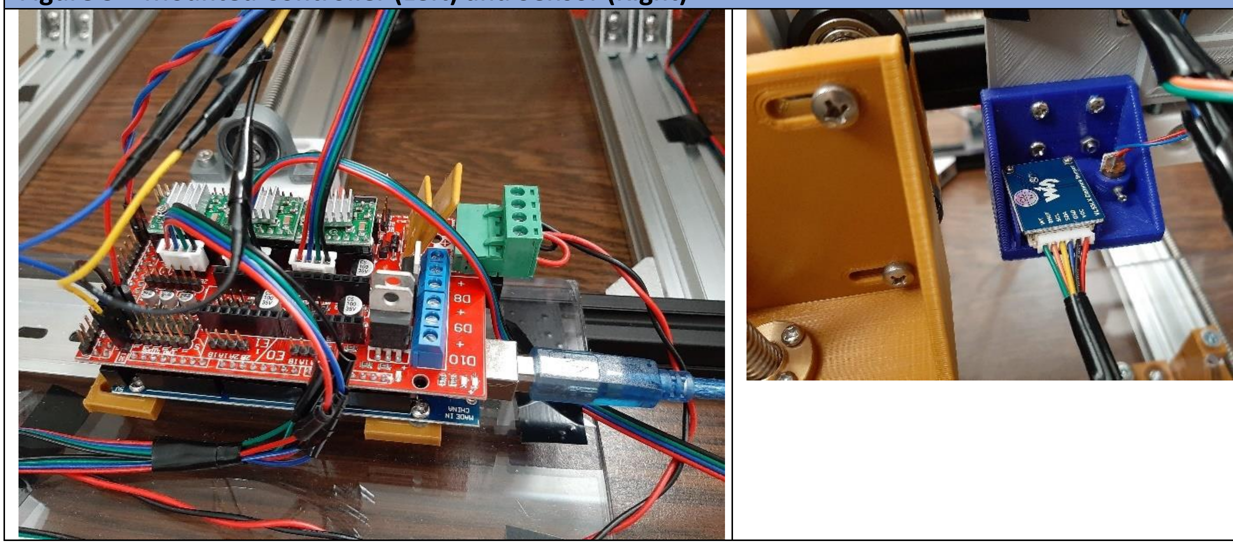

5 Firmware Design

Given the decision to use the Arduino Mega controller board, the control firmware would be written in the Arduino subset of C. Originally it was intended that this firmware would then communicate with a python based GUI over USB serial communication, which would allow the user to print files and communicate. However, due to a lack of time, communication and control was instead handled through the Arduino serial terminal via text-based serial commands. A list of these commands is included in the table below.

Table 4 – Software Commands and Keys		
Command	**Command Keys**	**Action/Notes**
Begin Control	<a>	Enables motor movement by future commands
+X movement	<b>	Move in the +X direction a distance equal to the default length (2mm at startup) at default speed rates (500mm/min at startup).
-X movement	<c>	Move in the -X direction a distance equal to the default length (2mm at startup) at default speed rates (500mm/min at startup).
+Y movement	<d>	Move in the +Y direction a distance equal to the default length (2mm at startup) at default speed rates (500mm/min at startup).
-Y movement	<e>	Move in the -Y direction a distance equal to the default length (2mm at startup) at default speed rates (500mm/min at startup).
+Z movement	<f>	Move in the +Z direction a distance equal to the default length (2mm at startup) at default speed rates (500mm/min at startup).
-Z movement	<g>	Move in the -Z direction a distance equal to the default length (2mm at startup) at default speed rates (500mm/min at startup).
Begin Profile	<h>	Move to profile Z location and X and Y zero coordinates and then begin scanning profile, performing a scanning measurement every 0.5mm.
Set Zero	<i>	Set the origin of the internal coordinate system to correspond to the current location.
Set Default Speed	<j>	Set the default speed in mm/min (e.g. typing "<j500>" will cause the new default speed to be set to 500mm/min).
Set Profile Y increment length	<k>	Set the profile Y increment length in mm (e.g. typing "<k0.5>" will cause the Y increment length to be set to 0.5mm).
Close Control	<l>	Disables motor movement by future commands.
Set Profile Z	<m>	Set the Z at which the machine will perform a scanning profile to the current Z location.
Set Default Length	<n>	Set the default length distance in mm (e.g. typing "<n10>" will cause the new default length to be set to 10mm).
Toggle (On or Off) positioning laser state.	<o>	Turn the positioning laser on or off.
Print Location and Z measurement	<p>	Prints the current location according to the internal coordinate system as well as the Z measurement from the laser.

6 Open-Loop Control Design

As stated previously, it was decided that encoders would not be used during this project. In accordance with this, it was therefore necessary to employ open loop stepper control. This is extremely typical in LSCNC control and can produce accurate results under low load conditions and low speeds [15]. Various aspects of the open-loop control design are described in the following sections

6.1 Trajectory Generation

The most common issues associated with the use of open loop stepper control at low speeds is ultra-high acceleration change, known as jerk causing step loss. This occurs whenever a non-smooth location is encountered on a velocity profile and is proportional to the instantaneous change in acceleration. To decrease the effect of jerk on the steppers CNC machines employ trajectory generation algorithms which attempt to increase velocity gradually at finite acceleration rates (see Equation 4 for suitable accelerations for this device). Figure 4 illustrates several different trajectory generation profiles. For simplicity sake this project will employ trapezoidal trajectory generation.

Equation 4 – Maximum stepper acceleration (adapted from [3])
Assumption: Because the Z-axis motors carry the greatest mass their acceleration will result in the greatest force experienced by the motor. $D\ [T8\ Diameter] = 8mm$ $Lead\ [T8\ Lead] = \frac{8mm}{360°}$ $m_{Xaxis}\ [estimated\ mass\ of\ X - axis\ assembly] = 1.233kg$ $n\ [number\ of\ motors] = 2$ $T_{mot}\ [motor\ Torque] = \ 0.40\ Nm$ $MA\ [Mech. Advantage]$ $VR\ [Velocity\ Ratio]$ $\xi\ [Efficiency] = 1\ (an\ assumption)$ $a_{max}\ [max\ acceleration] = ?$ $$MA = VR * \xi = \frac{\pi D}{Lead} = \pi$$ $$\frac{T_{mot} * n * 2}{D} = F_{Motor} = 200N$$ $$MA = \frac{F_{grav} + F_{accel}}{F_{Motor}} \rightarrow \frac{MA * F_{Motor}}{m} - g = a_{max} = 500\frac{m}{s^2} = 1.8 * 10^9 \frac{mm}{\min^2}$$ **Results: acceleration limit not likely to produce missed steps given the high max acceleration of the motors and the small attached masses.** **Calculation uses specs from Nema17 steppers [13]

Figure 4 – Trajectory generation types

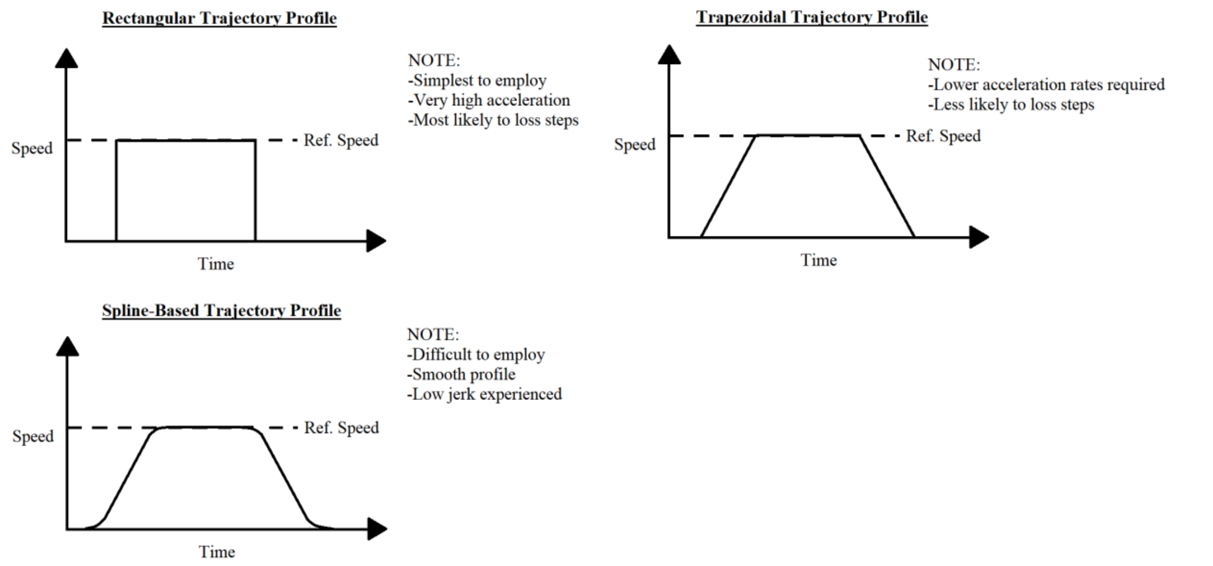

6.2 Practical Velocity Control of Steppers

Steppers are position controlled devices: each commanded pulse therefore produces 1 step of movement. The frequency of these pulses is directly proportional to the speed of the motor. Practically pulse frequency is handled by step delay. The conversion between desired motor speed and delay is derived in Equation 5.

Equation 5 – Conversion factor between velocity and step delay

Assumption: Code between pulses takes zero time. This is mostly validated because ultra-long tasks such as communication are disabled during movement.

$Min\ Res = 200 steps/mm$

$d[\mu s] = ?$

$v\left[\frac{mm}{min}\right] = ?$

$delay\ conv.factor = dcf\ = ?$

$$d[\mu s] = \frac{1}{v\left[\frac{mm}{min}\right]} * 1step * \frac{1}{MinRes\ \left[\frac{steps}{mm}\right]} * \frac{60s}{min} * \frac{1000000\mu s}{1s}$$

$$d[\mu s] * v\left[\frac{mm}{min}\right] = \mathbf{300000}\left[\frac{\boldsymbol{mm * \mu s}}{\boldsymbol{min}}\right] = \boldsymbol{dcf}$$

**Calculation uses specs from Nema17 steppers [13]

6.3 Scanning Profile Path

In order to scan the entire object a back-and-forth tool path strategy was employed in which the X-axis moved back-and-forth across the entire platform while the Y-axis moved forward a distance of *Profile-Y-Increment* with each pass. An illustration of this path is presented in Figure 5.

Figure 5 – Back-and-Forth path strategy (Profile-Y-Increment length here exaggerated)

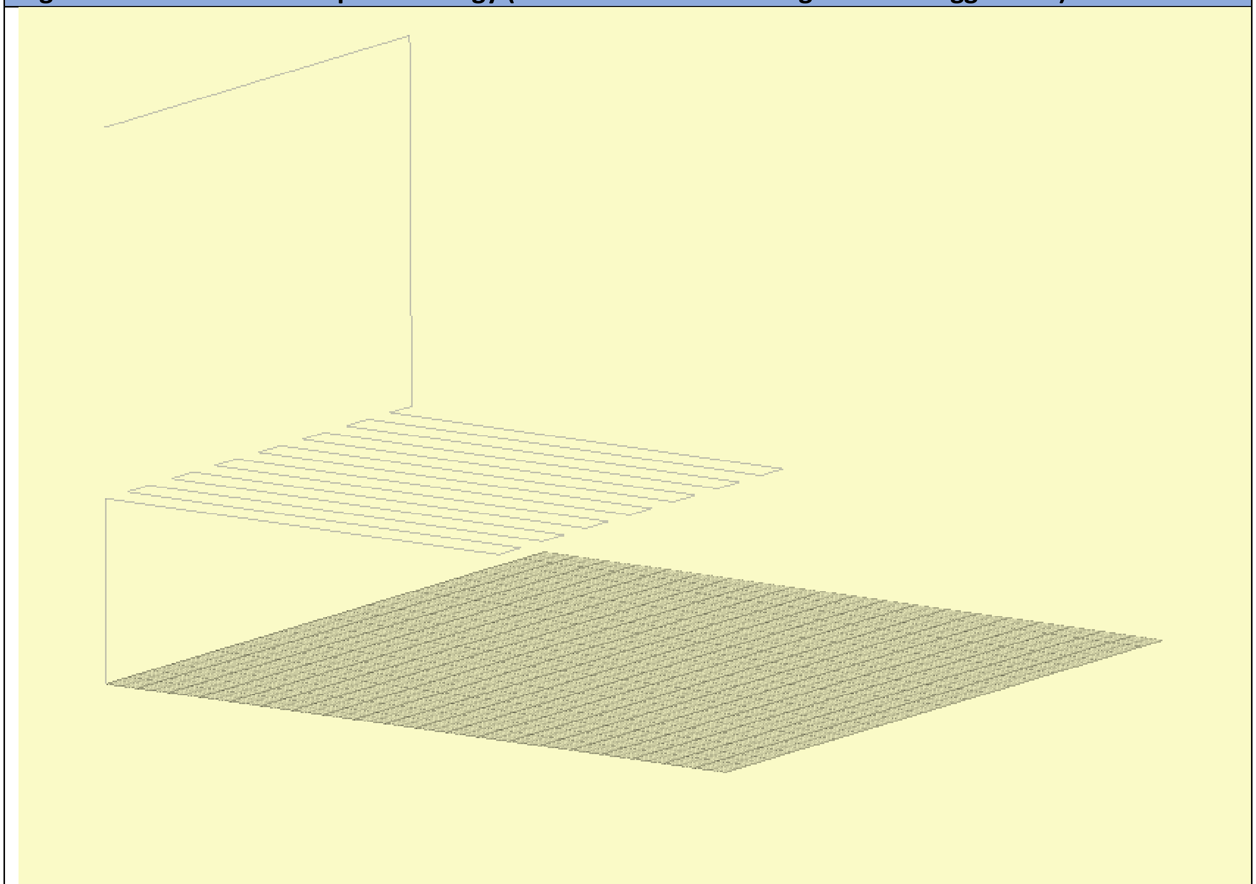

Every 0.5mm during this path the tool stops and takes a Z-measurement, thus creating a grid of reading of the QC part. Because all movements in this profile was taken along one of the principle axes of the workspace, diagonal and circular interpolation was not employed in the device control capabilities. Similarly, because all accelerations and decelerations begin and end (respectively) at zero, acceleration from one speed to another was not employed in the device control capabilities.

7 Final Assembly

After completing the design and assembly the firmware was uploaded and debugged. Measurements of the instrument revealed the build area to be slightly more than 127mm x 150mm x 150mm (X,Y,Z respectively). An image of the final assembly is displayed in Figure 6.

Figure 6 – Final assembly

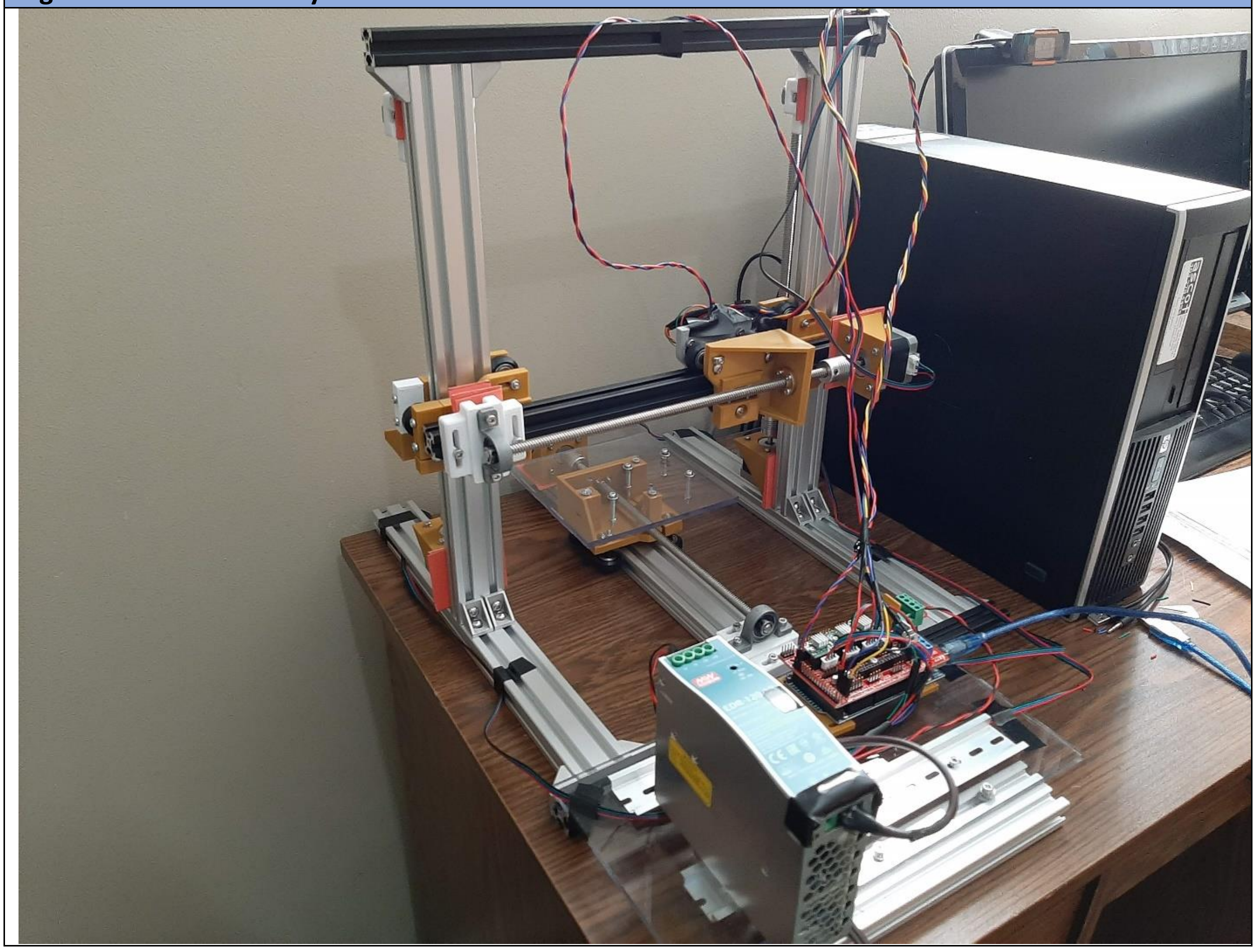

It should be noted that several modifications needed to be made in order make the QC CNC machine viable. First, no leveling mechanism had been considered for the threaded rods guiding each axis. This combined with the fact that by necessity the bars were over-constrained (guided through three separate parts on the rail) resulted in the bar not being parallel to each axis. In this prototype this issue was fixed by placing cardstock between the frame and brackets (red in the above picture). In future designs this will need to be accounted for using slots and spacers.

It was also noted during the construction that the ideal wheel spacing had been miscalculated. This resulted in several new slots needing to be drilled into the motor brackets for linear alignment. In future builds these slots should be formalized and added to the CAD files.

8 Testing Methodology

In order to perform the test the accuracy of the QC CNC machine, following tests would be employed.

8.1 VL53L0X Material Surface Test

As with most scanning techniques, the accuracy of the VL53L0X range finder module is affected by object surface qualities and light conditions [12]. To determine the optimal surface quality for the sensor the following test procedure was employed.

1. Three flat test objects were obtained:
   a. A lightly colored wooden board
   b. A mat black board
   c. A slightly reflective black box
2. Each was placed on a measurement board apparatus (see Figure 7) perpendicular to the VL53L0X 60mm away.
3. 100 readings were taken of each.
4. The average and standard deviation of each measurement cycle was examined.

Based on this experiment, the designer would augment the test piece to increase scanning accuracy.

Figure 7 – Measurement board apparatus

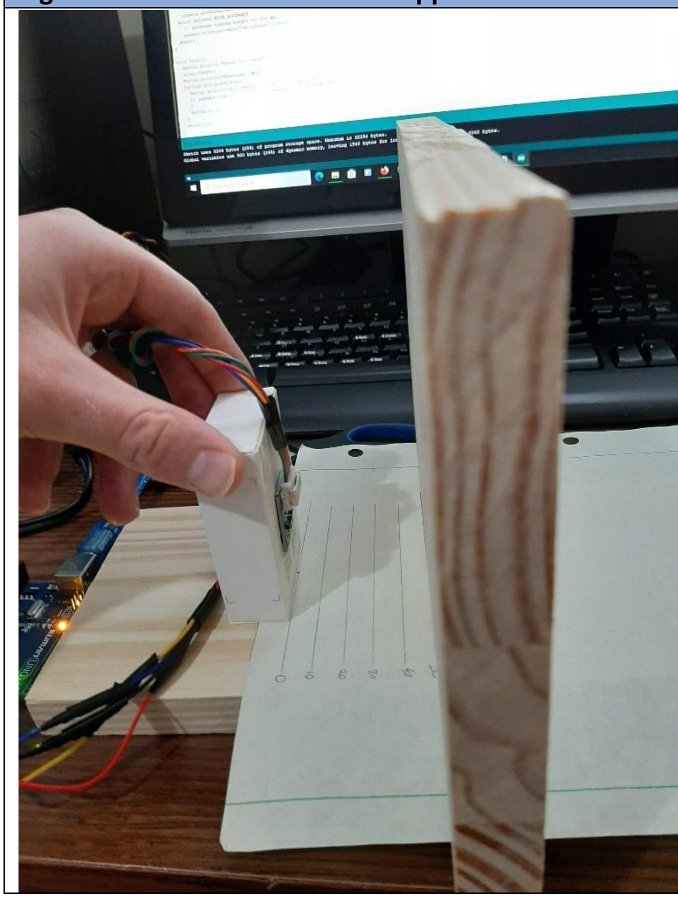

8.2 Surface Baseline Scanning Test

In order to isolate any issues related to the integration of the VL53L0X and the QC machine a test was conducted in order to view the scanning accuracy of the apparatus on a flat plane. To do this the VL53L0X was connected to the final assembly and the following test procedure was performed:

1. The *Profile-Y-Increment-Length* and the scanning increment were increased to 2mm to increase profile speed.
2. A black piece of construction paper was placed over the otherwise transparent platform and the lights were dimmed as much as possible (see Figure 8).
3. The machine was allowed to perform a profile and the results were compared against actual caliper measurements.

By performing this test, the designer hoped to get a baseline test against which other scans could be compared.

Figure 8 – Baseline scanning apparatus

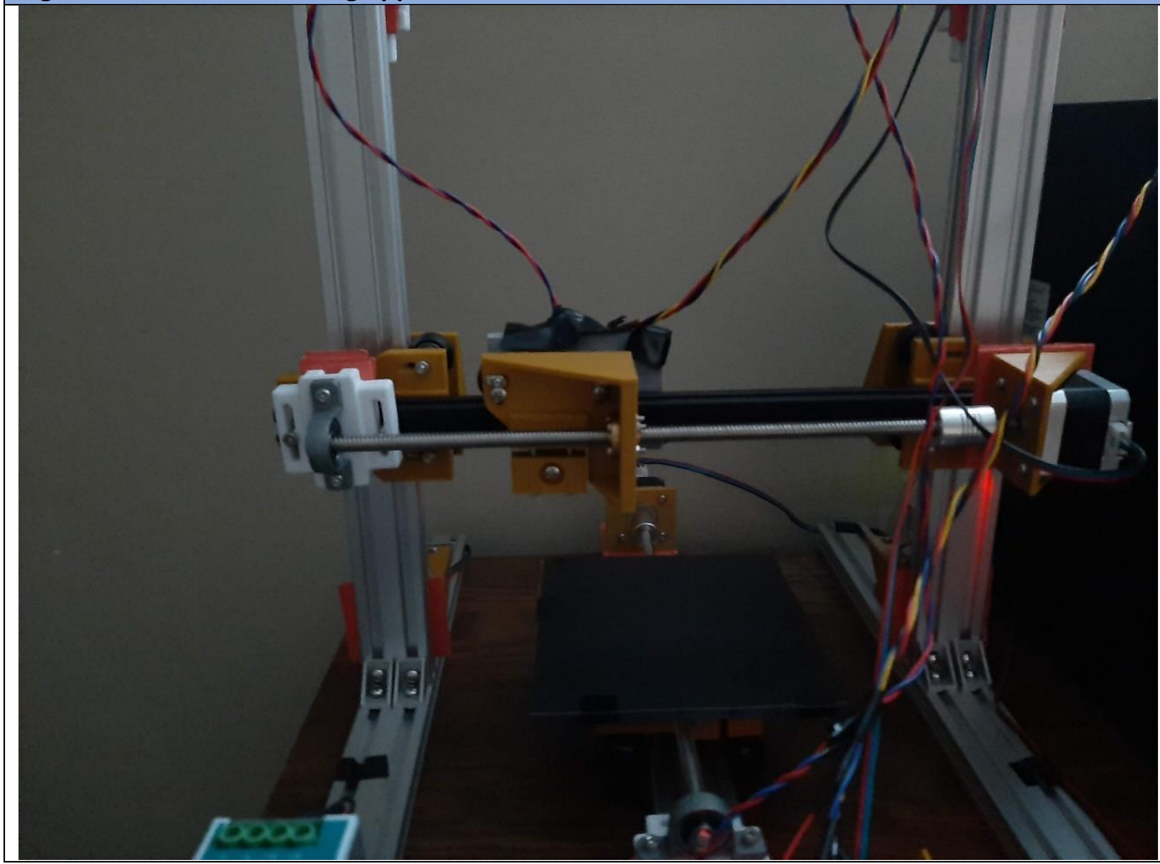

8.3 Test Piece Flaw Identification

During the final performance test, the designer needed to determine the ability of the machine to identify features accurately enough that further analysis could be performed. This test would also provide data concerning profile speed. To perform this test the following procedure was followed:

1. Two test pieces with slight differences were 3D printed (see Figure 9).
2. Any surface modifications recommended by the VL53L0X Material Surface Test were applied.
3. Unless otherwise determined to be an infeasible amount, both the *Profile-Y-Increment-Length* and the scanning increment length were reduced to 0.5mm
4. The 1st test piece was secured to the bed and scanned.
5. The 2nd test piece was secured and scanned.
6. The results of the two scans were compared to one another.

Figure 9 – Scan test pieces

9 Testing Results

9.1 VL53L0X Material Surface Test

During initial material testing of the VL53L0X the designer determined that the VL53L0X sensor had a minimum range at about 50mm, which was confirmed by the manufacturers page. Using this value in the field of view calculation is was calculated that the new laser diameter and minimum resolution would be 22mm and a measurement error of 1.5mm. This was of course too large for any serious measurements and would of course contribute significantly to the measurement error.

Table 5 – Material surface test data at 60mm

Surface Type	Average Value (mm)	Error (mm)	Standard Deviation (mm)
Wood	55.7	4.3	0.55
Shiny Black	48.4	11.6	0.8
Mat Black	57.9	2.1	0.8

It was also preliminarily observed that the mat black finished surface demonstrated the lowest overall error and therefore the test pieces were painted black in order to increase accuracy (see Figure 10). It was also noted that all of the surfaces displayed nearly the same standard deviation, leading the designer to believe that material surface differences could be compensated for using some sort of linear factor.

Figure 10 – Painted scan test pieces

9.2 Surface Baseline Scanning Test

After the completion of the testing the scan points were compiled into a PLY file and viewed using blender (see Figure 11). It should be noted that the scanner is not perfectly centered over the test plate, and therefore passes over and scans the desk underneath as well. This is observed both on the left and front of Figure 11

Figure 11 – Baseline plate scan and photo taken from the same angle

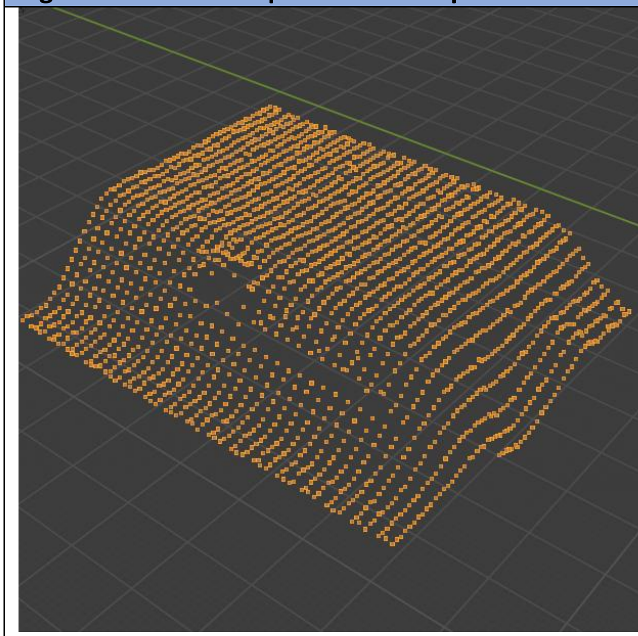

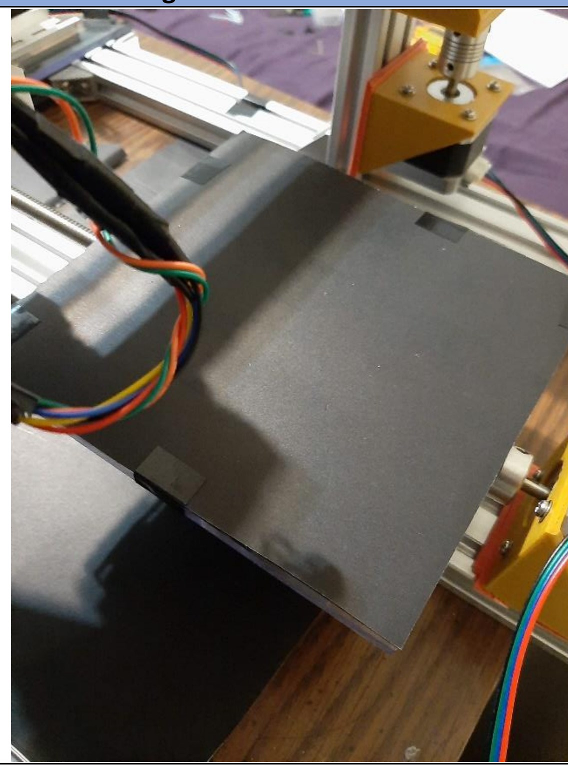

Several things were interpreted from this preliminary scan. First it was interpreted that the hypothesis of the designer that height differences in a laser area will be averaged was correct. The nearly diagonal surface observed occurs as the laser area begins to travel over the build plate and scans the desk surface. It can also be interpreted visually that error due to noise is extremely minimal, with only one small section showing significant noise readings. It should be noted that this noise reading corresponds to the location of some electrical tape with a higher reflective index than the covered plate.

9.3 Test Piece Flaw Identification

As stated in the test methodology, both painted test pieces were secured to the test bed. The results of these two scans can be seen in Figures 12 and 13. It should be noted that the scan of test piece 1 was taken at 104.7mm and in 2mm increments, but that during the scanning of test piece 2 these values were changed to 53.7mm and 1mm respectively to increase scan quality.

Figure 12 – Test piece one, scan and photo taken from same angle

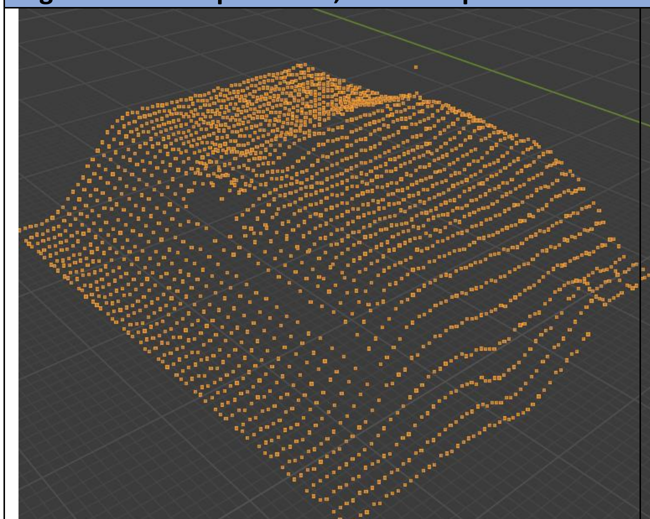

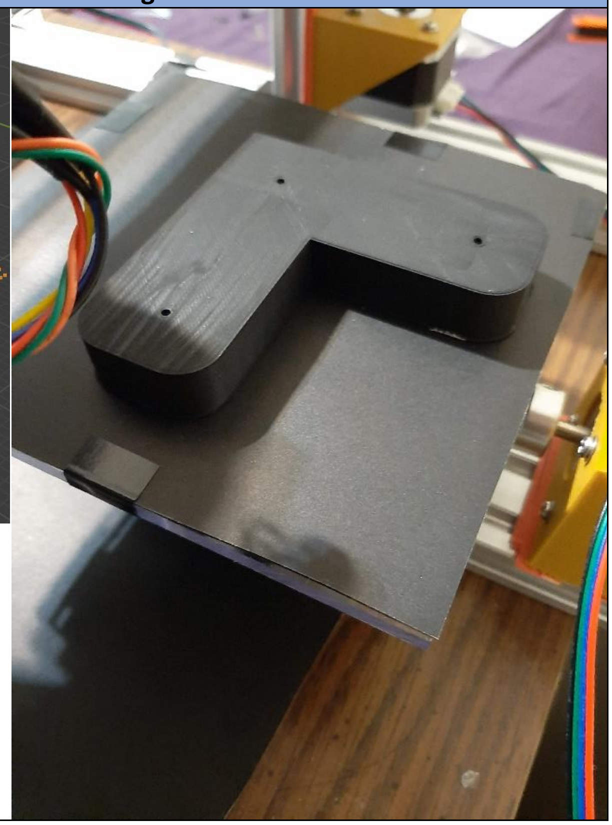

Figure 13 – Test piece two, scan and photo taken from same angle

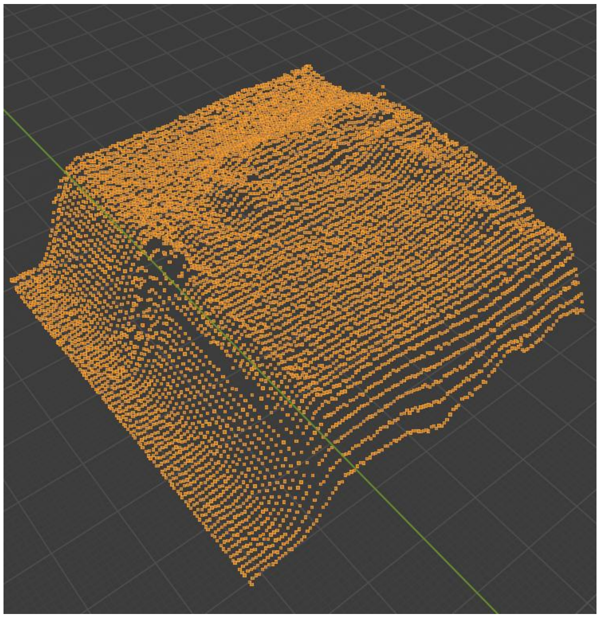

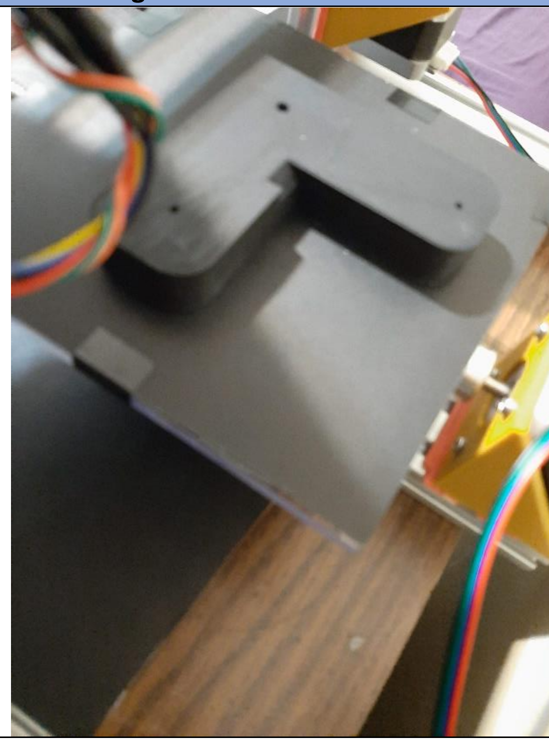

After viewing the scans, it was apparent to the designer that the size of the laser area was having a significant effect on the measurement quality. Despite this the outline of both test pieces could still be seen, and some noise and divoting did appear to be occurring around the holes of the 2nd test piece.

10 Discussion

The purpose of this design project was to create a prototype scanner with high enough accuracy to be usable in quality control applications. Additional this scanner would be low-cost and perform a scan in under five minutes. A summary of these goals and the resulting behavior of the designed prototype are contained in Table 6.

Table 6 – Design goals and prototype performance comparison

Goal	**Units**	**Goal Range**	**Prototype Performance**
Cost of functioning prototype	$	<1000	~$950
Speed of QC Process	Min	<4	25-40
Z-Height Accuracy	mm	±0.1	1.5 (theoretical)
X/Y Resolution	mm	<1	22
Time Frame	Dates	May 1 – August 7, 2020	Complete on time

Using these goals as failure criteria, the designer concludes that, due to the lack of a sufficiently accurate laser measurement device, this prototype was not able to successfully fulfill its goals.

The resulting failure of this project is despite the fact that the mechanical construction of the LSCNC machine, the custom control firmware, and the electronics used were sufficiently robust to achieve the above performance goals (with accurate movement resolution theoretically at 0.005mm). Therefore it is the recommendation of the designer that future QC CNC machines simply employ a more accurate laser sensor such as an industrial sensor [9] or a more appropriately sized low-cost sensor (such as the VL6180X with a range of 0-100mm [16]) as the main issue associated with the sensor used was that its laser area was too large at its minimum distance.

Pertaining to the incredibly long scan time, it was noted by the designer that because the motors and range sensor were being operated by the same single processor board, the entire system needed to stop every time a measurement was taken (each measurement taking about 20ms). Therefore, in order to decrease the scanning time the designer also recommends that the single controller system be replaced with an I2C integrated multi-board system, in which the main controller handles movement, while the second board takes measurements, tracks motion using motor encoders, and reports these values via serial to the serial terminal. By doing this a future QC CNC machine would be able to maintain continuous movement while continuing to scan, if the speed of movement is significantly slower than the speed of measurement.

11 Conclusion

The purpose of this project was to design a prototype QC CNC machine using LSCNC parts and off the shelf electronics which was sufficiently accurate to be used in industrial settings. Using off the shelf components, the designer was able to create and build a custom LSCNC QC machine, however due to the poor quality of the purchased sensor the machine was not able to fulfill its scan accuracy goals. The designer recommends that future iterations of this project employ a more accurate sensor and a more complex board configuration in order to meet the design goals.

12 References

[1] Q. Feng and K. C. Kapur, “Quality Engineering: Control, Design and Optimization,” 01-Jan-1970. [Online]. Available: https://link.springer.com/chapter/10.1007/978-1-84800-131-2_13. [Accessed: 15-Aug-2020].

[2] L. Carolo, “3D Printer Axis: The Basics – Simply Explained,” *All3DP*, 22-May-2020. [Online]. Available: https://all3dp.com/2/3d-printer-axis-the-basics-simply-explained/. [Accessed: 15-Aug-2020].

[3] “Screw Threads & Mechanical Advantage,” *Kelston Actuation*. [Online]. Available: https://www.kelstonactuation.com/knowledge/screw-threads-and-mechanical-advantage. [Accessed: 15-Aug-2020].

[4] D. Florian, “How to Build a 3D Printer: Linear Rails,” *Building a 3D Printer: Linear Rails*. [Online]. Available: https://www.drdflo.com/pages/Guides/How-to-Build-a-3D-Printer/Linear-Rail.html. [Accessed: 15-Aug-2020].

[5] W. Gastreich, “Stepper Motors Advantages and Disadvantages,” *RealPars*, 22-Jul-2020. [Online]. Available: https://realpars.com/stepper-motors-advantages/. [Accessed: 15-Aug-2020].

[6] H. Kondo, “3D Printer Layer Shifting: 3 Easy Ways to Avoid It,” *All3DP*, 15-Dec-2019. [Online]. Available: https://all3dp.com/2/layer-shifting-3d-printing-tips-tricks-to-solve-it/. [Accessed: 15-Aug-2020].

[7] A. HartCarroll, “11 Best 3D Printer Controllers Reviewed with Buying Guide,” *VeryCreate.com*, 19-May-2020. [Online]. Available: https://verycreate.com/best-3d-printer-controller/. [Accessed: 15-Aug-2020].

[8] “ProductivityOpen: Open-Source Agility Meets Industrial-Grade Toughness,” *AutomationDirect*. [Online]. Available: https://www.automationdirect.com/open-source/home. [Accessed: 15-Aug-2020].

[9] “Micro-head Spectral-interference Laser Displacement Meter,” *Micro-head Spectral-interference Laser Displacement Meter - SI-F series | KEYENCE America*. [Online]. Available: https://www.keyence.com/products/measure/spectral/si-f/. [Accessed: 15-Aug-2020].

[10] S. Ibaraki, Y. Kimura, Y. Nagai, and S. Nishikawa, “Formulation of Influence of Machine Geometric Errors on Five-Axis On-Machine Scanning Measurement by Using a Laser Displacement Sensor,” *Journal of Manufacturing Science and Engineering*, vol. 137, no. 2, 2015.

[11] M. Deans, “To Probe or Not to Probe: Ending the Probing Debate,” *Fusion 360 Blog*, 10-May-2018. [Online]. Available: https://www.autodesk.com/products/fusion-360/blog/probe-not-probe/. [Accessed: 15-Aug-2020].

[12] “VL53L0X,” *STMicroelectronics*. [Online]. Available: https://www.st.com/en/imaging-and-photonics-solutions/vl53l0x.html. [Accessed: 15-Aug-2020].

[13] "17HS4401 Datasheet," *17HS4401 Datasheet PDF - Datasheet4U.com*. [Online]. Available: https://www.datasheet4u.com/datasheet-pdf/MotionKing/17HS4401/pdf.php?id=928661. [Accessed: 15-Aug-2020].

[14] J. Kordik, "Open-loop System vs. Closed-loop System," *Motion Control Tips*, 06-Jul-2016. [Online]. Available: https://www.motioncontroltips.com/open-loop-stepper-motor-versus-closed-loop-stepper-motor-systems/. [Accessed: 15-Aug-2020].

[15] "Stepper Motors - Everything You Need to Know About Stepper Motors," *Oriental Motor U.S.A. Corp.* [Online]. Available: https://www.orientalmotor.com/stepper-motors/technology/everything-about-stepper-motors.html. [Accessed: 15-Aug-2020].

[16] "VL6180X," *STMicroelectronics*. [Online]. Available: https://www.st.com/en/imaging-and-photonics-solutions/vl6180x.html. [Accessed: 15-Aug-2020].